Research Article

Application of High-Throughput Transcriptomics for Mechanism-Based Biological Read-Across of Short-Chain Carboxylic Acid Analogues of Valproic Acid

Nanette G. Vrijenhoek[1], Matthias M. Wehr[2], Steven J. Kunnen[1], Lukas S. Wijaya[1], Giulia Callegaro[1], Martijn J. Moné[1], Sylvia E. Escher[2] and Bob van de Water[1]

[1]Leiden Academic Centre of Drug Research, Leiden University, Leiden, The Netherlands; [2]ITEM, Fraunhofer Institute, Hannover, Germany

Abstract

Chemical read-across is commonly evaluated without specific knowledge of the biological mechanisms leading to observed adverse outcomes *in vivo*. Integrating data that indicate shared modes of action in humans will strengthen read-across cases. Here we studied transcriptomic responses of primary human hepatocytes (PHH) to a large panel of carboxylic acids to include detailed mode-of-action data as a proof-of-concept for read-across in risk assessment. In rodents, some carboxylic acids, including valproic acid (VPA), are known to cause hepatic steatosis, whereas others do not. We investigated transcriptomics responses of PHHs exposed for 24 h to 18 structurally different VPA analogues in a concentration range to determine biological similarity in relation to *in vivo* steatotic potential. Using a targeted high-throughput screening assay, we assessed the differential expression of ~3,000 genes covering relevant biological pathways. Differentially expressed gene analysis revealed differences in potency of carboxylic acids, and expression patterns were highly similar for structurally similar compounds. Strong clustering occurred for steatosis-positive versus steatosis-negative carboxylic acids. To quantitatively define biological read-across, we combined pathway analysis and weighted gene co-expression network analysis. Active carboxylic acids displayed high similarity in gene network modulation. Importantly, free fatty acid synthesis modulation and stress pathway responses are affected by active carboxylic acids, providing coherent mechanistic underpinning for our findings. Our work shows that transcriptomic analysis of cultured human hepatocytes can reinforce the prediction of liver injury outcome based on quantitative and mechanistic biological data and support its application in read-across.

1 Introduction

There is a need for new approach methodologies (NAMs) for chemical safety assessment that will complement existing and future requirements for non-animal based testing for next generation risk assessment (Kavlock et al., 2018; Pistollato et al., 2021). Therefore, read-across assessment and integrated approaches to testing and assessment (IATAs) in the context of adverse outcome pathways (AOPs) are implemented in toxicity testing strategies (Escher et al., 2019; Rovida et al., 2021). Read-across among compounds is commonly used for "gap-filling" of target compounds by studying effects of structurally similar source compounds (Schultz et al., 2015). In routine chemical read-across, however, knowledge of biological mechanisms is lacking. In contrast, AOPs are frameworks to organize mechanistic knowledge and information regarding biological processes that lead to an adverse event, but it is time-consuming and data-demanding to build AOPs. The application of AOPs in toxicity testing is supporting IATAs in regulatory decision-making (Patlewicz et al., 2014; Tollefsen et al., 2014; Vinken, 2015). Furthermore, toxicity test systems are being developed for high-throughput screening, allowing testing of numerous compounds at multiple concentrations. Such biological assays aim to unravel the mode-of-action (MoA) underlying adverse events, contributing to AOP development and assessing similarities in MoA among compounds. Transcriptomic

Received July 26, 2021; Accepted December 16, 2021;
Epub January 17, 2022; © The Authors, 2022.

ALTEX 39(2), 207-220. doi:10.14573/altex.2107261

Correspondence: Bob van de Water, PhD
Division of Drug Discovery and Safety, Leiden Academic Centre for Drug Research
Leiden University, Einsteinweg 55, 2333 CC Leiden, The Netherlands
(b.water@lacdr.leidenuniv.nl)

techniques are continuously developed to be more cost-effective and less time-consuming, allowing high-throughput gene expression profiling of multiple compounds at different concentrations in parallel (Mav et al., 2018; Gwinn et al., 2020; Harrill et al., 2021). The combination of these techniques has already proven a robust method to quantify concentration-dependent chemical-induced transcriptomic responses for a panel of different liver toxicants in HepaRG cells (Ramaiahgari et al., 2019).

Here, we combined a biological similarity study with physicochemical data, transcriptomic data and information on the *in vivo* adverse outcome using 18 structurally similar carboxylic acids. It was our premise that unravelling the cellular MoA could eventually strengthen a read-across assessment. Hereto, we performed transcriptomic analysis on the entire panel of 18 carboxylic acids. One widely studied carboxylic acid is valproic acid (VPA), an anticonvulsant with a potential for liver toxicity. Since the MoA of VPA is largely known and an AOP of drug-induced liver steatosis has been established (van Breda et al., 2018), we were able to systematically assess whether other carboxylic acids induce mechanistically similar pathway responses. Furthermore, a selection of these short-chain fatty acids (SCFA) has previously been tested in animals and also caused liver steatosis. Therefore, we anticipated that different carboxylic acids might demonstrate a similar transcriptomic response, albeit with different potency. We used primary human hepatocytes (PHH) as the test system and deployed the Toxicogenomics-MAPr tool (TXG-MAPr; Callegaro et al., 2021) to derive toxicological fingerprints induced by carboxylic acids. This tool allows a rapid quantitative mechanistic understanding of transcriptomic data based on weighted gene co-expression network analysis (WGCNA) of the TG-GATEs database. In short, the TXG-MAPr consists of modules, which are gene co-expression networks based on the gene expression data of PHHs exposed to more than 150 compounds and available in the TG-GATEs database. These modules are also annotated with functional information including pathway annotation and transcription factor enrichment. The eigengene (EG) score summarizes the log2 fold change (log2FC) of the genes within a module, and this is also reflected in the size and color of a module circle in the TXG-MAPr. The gene that has the highest correlation between the log2FC and the module EG score is called a hub gene, and this gene is the most representative of the entire module. The TXG-MAPr tool has a feature for uploading new transcriptomic data, which is used to calculate gene sub-network (module) perturbations captured in a module EG score. We compared our data with VPA expression profiles from the TG-GATEs database and with full-transcriptome panels generated in HepG2 cell lines. Finally, stress pathway responses, involved in many toxicological responses, were investigated.

2 Materials and methods

Cell culture

PHHs (LiverPool™ 10-donor mixed gender pooled cryoplatable human hepatocytes, Cat No. X008001-P) were acquired from BioReclamationIVT. Upon thawing, cells were diluted in warm thawing medium (SEKISUI XenoTech OptiThaw Hepatocyte Media, Cat No. K8000) and centrifuged for 10 min at 100 g. Cells were resuspended in InVitroGro CP medium (BioIVT, Cat no. Z99029) supplemented with Torpedo™ antibiotics mix (BioIVT, Cat no. Z99000) and plated in clear 96-well plates precoated with collagen (Corning, Cat no. 10469602) at 70,000 cells per well. 8 hours after plating, the medium was replaced with InVitroGro HI medium (BioIVT, Cat no. Z99009) supplemented with Torpedo™ mix. One day after plating, cells were chemically exposed to carboxylic acids in supplemented InVitroGRO™ HI medium.

HepG2 cells were acquired from ATCC (clone HB8065). They were maintained and exposed in high-glucose DMEM supplemented with 10% (v/v) FBS, penicillin (25 U/mL) and streptomycin (25 µg/mL). Cells were used between passage 12 and 15 and plated at 50,000 cells per well in clear 96-well plates. One day after plating, cells were exposed to carboxylic acids.

Reagents and exposures

All carboxylic acids were acquired from Sigma Aldrich except for 2-propylheptanoic acid (Endeavour Speciality Chemicals Ltd) and 2-ethylpentanoic acid (Santa Cruz) through the EU-ToxRisk consortium. These compounds and their characteristics are summarized in Table 1. All treatments were freshly prepared on the day of exposure and were accompanied with DMSO in a final treatment concentration of 0.1%. The concentration range of the exposures for all compounds and in all cell types, except samples measured for whole transcriptome, was 0.2 mM and a log2 scale of 6 concentrations (0.5 to 16 mM). The 0.2 mM concentration was included in the range of all compounds since a concentration around the cmax was desired (cmax: maximum concentration of VPA detected in plasma in patients (Huppelschoten, 2017)). To compare gene expression between TempO-seq EU-ToxRisk 2.2 gene set and whole transcriptome gene set, in a separate experiment HepG2 cells were exposed to VPA in a concentration range of 0.12, 0.6, 1.2, 2.4, 4.9, 7.3 mM. Exposure time for all treatments for EU-ToxRisk 2.2. gene set was 24 h; but for the HepG2 whole transcriptome gene set samples were obtained at both 8 h and 24 h. All data is from 3 independent biological replicates. For the negative control (0.1% DMSO) condition, 3 technical replicates per biological replicate were pooled and sequenced as 1 sample.

Abbreviations
AOP, adverse outcome pathway; CR, concentration response; DEGs, differentially expressed genes; EG, eigengene; FC, fold change; HDAC, histone deacetylase; GO, gene ontology; IATA, integrated approaches to testing and assessment; MACCS, Molecular ACCess System; MCFA, medium-chain fatty acids; MoA, mode-of-action; NAMs, new approach methodologies; PHH, primary human hepatocyte; PS, potency score; SCFA, short-chain fatty acids; TG-GATEs, Toxicogenomics Project-Genomics Assisted Toxicity Evaluation System; TXG-MAPr, Toxicogenomics-MAPr; VPA, valproic acid; WGCNA, weighted gene co-expression network analysis

Tab. 1: Carboxylic acids

Name	CAS	Abbre-viation	Structure (SMILES)	Structural similarity relative to VPA	Chain length at position 2	Branched	Steatosis *in vivo* data	References
Valproic acid	99-66-1	VPA	CCCC(CCC)C(=O)O	1	3.3.0	branched	positive	Espandiari et al., 2008; Tong et al., 2005; Sugimoto et al., 1987; Löscher, 1992; Abdel-Dayem, 2014; Knapp, 2008; Ibrahim, 2012; Acosta, 2012
2-Propyl-heptanoic acid	31080-39-4	2PHP	CCCCCC(CCC)C(=O)O	0.97	5.3.0	branched	unknown	
2-Ethyl-heptanoic acid	3274-29-1	2EHPA	CCCCCC(CC)C(=O)O	0.97	5.2.0	branched	unknown	
2-Propyl-hexanoic acid	3274-28-0	2PHA	CCCCC(CCC)C(=O)O	0.97	4.3.0	branched	unknown	
2-Ethyl-hexanoic acid	149-57-5	EHXA	CCCCC(CC)C(=O)O	0.97	4.2.0	branched	positive	Juberg et al., 1998; Szilagyi, 2012
2-Ethyl-pentanoic acid	20225-24-5	EPA	CCCC(CC)C(=O)O	0.94	3.2.0	branched	unknown	
2-Methyl-hexanoic acid	4536-23-6	2-MHXA	CCCCC(C)C(=O)O	0.91	4.1.0	branched	unknown	
2-Propyl-4-pentenoic acid (4-ene VPA)	1575720	2EVPA	CCCC(CC=C)C(=O)O	0.89	3.3.0	branched	positive	Tang, 1995; Baillie, 1992
Octanoic acid (caprylic acid)	124072	OCT	CCCCCCCC(=O)O	0.89	6.0.0	unbranched	negative	Szilagyi, 2012
2-Methyl-pentanoic acid	97-61-0	MPA	CCCC(C)C(=O)O	0.88	3.1.0	branched	unknown	Szilagyi, 2012
Hexanoic acid (caproic acid)	142-62-1	HEX	CCCCCC(=O)O	0.86	4.0.0	unbranched	negative	Szilagyi, 2012
2-Ethyl-1-hexanol	104767	2E1H	CCCCC(CC)CO	0.81	4.2.0	branched	positive	Semino, 1998
2-Methyl-butyric acid	1730-91-2	MBUT	CC[C@H](C)C(=O)O	0.8	2.1.0	branched	unknown	
2.2-Dimethyl-pentanoic acid	1185393	2.2MPA	CCCC(C)(C)C(=O)O	0.79	3.1.1	branched	unknown	
4-Pentenoic acid	591800	4PA	C=CCCC(=O)O	0.78	3.0.0	branched	positive	Thayer, 1984; Yuge, 1990; Tang et al., 1995; Baillie, 1992
2-Ethyl-butyric acid	88-09-5	2EB	CCC(CC)C(=O)O	0.73	2.2.0	branched	negative	Szilagyi, 2012
Propionic acid	79094	PROP	CCC(=O)O	0.62	2.0.0	unbranched	negative	Szilagyi, 2012
Pivalic acid	75-98-9	PIV	CC(C)(C)C(=O)O	0.53	1.1.1	branched	negative	IUCLID, Shell Netherlands, 1990

Annotation of carboxylic acids

Carboxylic acids were annotated by the following parameters: steatosis induction, chain length, branching, and VPA-similarity. Steatosis induction was determined by literature research and previously reported (Escher et al., 2021). Chain length was determined by counting Cs from the 2nd C from the acid group. Branched carboxylic acids have 2 or more chains from the 2nd C. VPA similarity scores of all analogues relative to the target compound were calculated using the MACCS (Molecular ACCess System) fingerprint from RDKit and DICE algorithm, where 1 is VPA and 0.53 is most dissimilar to VPA in our compound set (Tab. 1).

Transcriptomics

After 24 h of compound exposure, cells were washed with PBS and lysed with 50 µL 1x BNN lysis buffer (BioClavis, Glasgow, Scotland) diluted in PBS. After 15 min at RT, the lysate was frozen at -80°C and shipped to BioClavis, where lysates were analyzed using TempO-Seq technology, deploying either the S1500+ gene set (Mav et al., 2018) plus additional genes, together called EU-ToxRisk 2.2 (Tab. S1[1]) for the PHH and HepG2 samples, referred to as S1500+ set in the manuscript for the PHH and HepG2 samples, or the whole transcriptome gene set (manifest supplied in Tab. S1[1]). Probe alignment for EU-ToxRisk 2.2 gene set and whole transcriptome gene set was performed by BioClavis (Yeakley et al., 2017; Limonciel et al., 2018; Yang et al., 2020). Briefly, FASTQ files were aligned using Bowtie, allowing for up to 2 mismatchings in the target sequence. This bioinformatics pipeline contained several quality controls with mapped/unmapped reads, replicate clustering, and sample clustering (Yeakley et al., 2017). When samples passed these tests, result count tables were ready for analysis.

Statistical analysis

Read counts of all probes were analyzed by an in-house pipeline using R (Fig. S1[1]). Data wrangling was done with packages reshape (Wickham, 2007), tidyr[2], and dplyr[3]. First, we performed a quality control on the transcriptomic data. Hereto, we analyzed the library size and count distribution of the dataset. Samples with a library size below 500k were discarded, since they were visibly clear outliers from the library size boxplots and may not represent a complete transcriptomic response (Fig. S2A[1]).

Variance of the probes followed an unequal bimodal histogram, suggesting that part of the probe set was not activated by any of the compounds (Fig. S2B[1]). Probes with overall variance below 1 were discarded since no variance indicated no changes in those genes in the whole dataset. They were excluded from DEG calculations to strengthen the significance of genes with higher variability in their expression, leaving ~2,700 genes.

For DEG calculation of targeted transcriptomics, we used the same approach as for RNA-seq data, which can be analyzed by the DESeq2 package, which is based on a negative binomial regression model (Love et al., 2014). Therefore, we checked and confirmed a negative binomial distribution in our targeted transcriptome data by plotting the pooled variance with package edgeR (Robinson et al., 2010) (Fig. S1C[1]).

In the analysis of samples sequenced with the whole transcriptome, no probes were discarded. Counts were normalized to counts per million. All chemical-treated samples were compared to the DMSO control treated samples to calculate the log-2FC and p-values with the DESeq2 package. DEGs had a p-adjusted value of < 0.05 and $|\log2FC| > 1.5$ unless otherwise stated (Fig. S1[1]). FCs and adjusted p-values were uploaded to the TXG-MAPr tool[4] (Callegaro et al., 2021), whereupon EG scores of the modules were extracted. Stress pathway target genes of the TempO-Seq data were extracted from the DoRothEA database, containing transcription factor-target interactions (Garcia-Alonso et al., 2019). Interactions are assigned levels ranging from A-E, where A is highest and E is lowest confidence. Levels ABC were used to extract target genes of corresponding stress pathway transcription factors.

All figures were made with either the R packages ggplot[5], UpSetR[6] or pheatmap[7], or the TXG-MAPr tool (Callegaro et al., 2021) and assembled in Adobe Illustrator V25.2.

Fig. 1 (see the next page): Differentially expressed genes in response to carboxylic acid exposure

A) Vulcano plots displaying DEGs for VPA-treated PHHs. B) Dose response graphs for the number of DEGs in response to all carboxylic acids. Red = significantly upregulated, blue = significantly downregulated. Similarity indicates structural similarity to VPA; steatosis indicates *in vivo* potential. PS = potency score, which is the sum of all DEGs in a concentration response (CR). C) Unique genes overlapping at a concentration of 4 mM. Set size indicates the total amount of DEGs. Green dots mark the treatment for each set of unique genes, which is quantified in the intersection size. Linked dots represent overlapping genes among multiple treatments. D) Heatmap showing the top 50 probes upregulated for VPA at 4 mM for all carboxylic acids. Darker blue in the similarity annotation means more similar to VPA, light-dark green indicates concentration range. Purple colors reflect the potency score of B. The genes with probe number are displayed vertically.

1 doi:10.14573/altex.2107261s

2 tidyr: Tidy Messy Data. https://cran.r-project.org/package=tidyr

3 dplyr: A Grammar of Data Manipulation. https://cran.r-project.org/package=dplyr

4 https://txg-mapr.eu/WGCNA_PHH/TGGATEs_PHH/

5 ggplot2: Elegant Graphics for Data Analysis. Springer-Verlag New York. https://ggplot2.tidyverse.org

6 UpSetR: A More Scalable Alternative to Venn and Euler Diagrams for Visualizing Intersecting Sets. https://cran.r-project.org/package=UpSetR

7 pheatmap: Pretty Heatmaps. https://cran.r-project.org/package=pheatmap

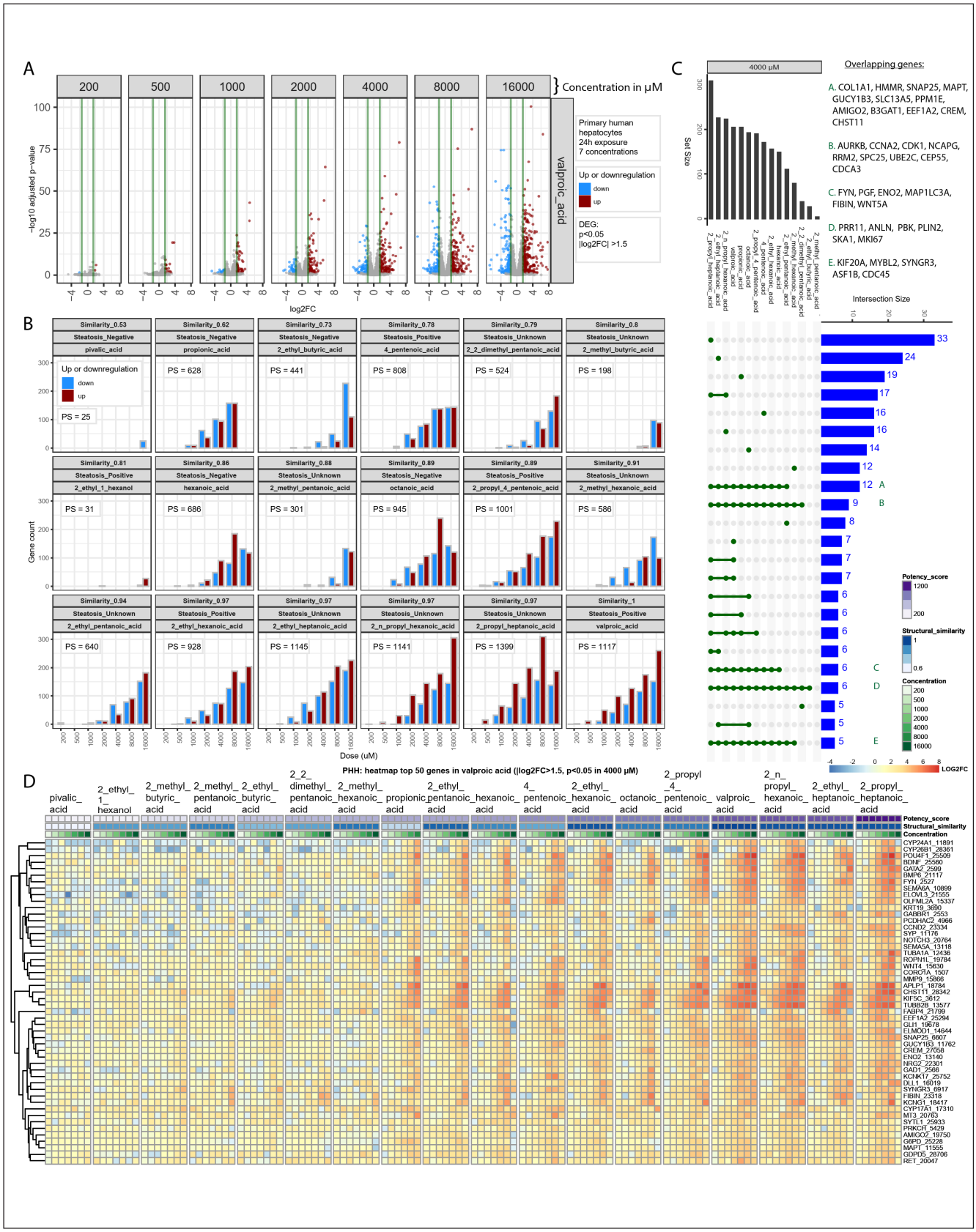
A
200
500
1000
2000
4000
8000
16000
Concentration in µM
−log10 adjusted p−value
log2FC
valproic_acid
Primary human hepatocytes
24h exposure
7 concentrations
Up or downregulation
down
up
DEG:
p<0.05
|log2FC| >1.5
B
Gene count
Dose (uM)
Up or downregulation
down
up
Similarity_0.53
Steatosis_Negative
pivalic_acid
PS = 25
Similarity_0.62
Steatosis_Negative
propionic_acid
PS = 628
Similarity_0.73
Steatosis_Negative
2_ethyl_butyric_acid
PS = 441
Similarity_0.78
Steatosis_Positive
4_pentenoic_acid
PS = 808
Similarity_0.79
Steatosis_Unknown
2_2_dimethyl_pentanoic_acid
PS = 524
Similarity_0.8
Steatosis_Unknown
2_methyl_butyric_acid
PS = 198
Similarity_0.81
Steatosis_Positive
2_ethyl_1_hexanol
PS = 31
Similarity_0.86
Steatosis_Negative
hexanoic_acid
PS = 686
Similarity_0.88
Steatosis_Unknown
2_methyl_pentanoic_acid
PS = 301
Similarity_0.89
Steatosis_Negative
octanoic_acid
PS = 945
Similarity_0.89
Steatosis_Positive
2_propyl_4_pentenoic_acid
PS = 1001
Similarity_0.91
Steatosis_Unknown
2_methyl_hexanoic_acid
PS = 586
Similarity_0.94
Steatosis_Unknown
2_ethyl_pentanoic_acid
PS = 640
Similarity_0.97
Steatosis_Positive
2_ethyl_hexanoic_acid
PS = 928
Similarity_0.97
Steatosis_Unknown
2_ethyl_heptanoic_acid
PS = 1145
Similarity_0.97
Steatosis_Unknown
2_n_propyl_hexanoic_acid
PS = 1141
Similarity_0.97
Steatosis_Unknown
2_propyl_heptanoic_acid
PS = 1399
Similarity_1
Steatosis_Positive
valproic_acid
PS = 1117
C
4000 µM
Set Size
Intersection Size
Overlapping genes:
A. COL1A1, HMMR, SNAP25, MAPT, GUCY1B3, SLC13A5, PPM1E, AMIGO2, B3GAT1, EEF1A2, CREM, CHST11
B. AURKB, CCNA2, CDK1, NCAPG, RRM2, SPC25, UBE2C, CEP55, CDCA3
C. FYN, PGF, ENO2, MAP1LC3A, FIBIN, WNT5A
D. PRR11, ANLN, PBK, PLIN2, SKA1, MKI67
E. KIF20A, MYBL2, SYNGR3, ASF1B, CDC45
Potency_score
Structural_similarity
Concentration
LOG2FC
D
PHH: heatmap top 50 genes in valproic acid (|log2FC>1.5, p<0.05 in 4000 µM)
pivalic_acid
2_ethyl_1_hexanol
2_methyl_butyric_acid
2_methyl_pentanoic_acid
2_ethyl_butyric_acid
2_2_dimethyl_pentanoic_acid
2_methyl_hexanoic_acid
propionic_acid
2_ethyl_pentanoic_acid
4_pentenoic_acid
2_ethyl_hexanoic_acid
octanoic_acid
2_propyl_4_pentenoic_acid
valproic_acid
2_n_propyl_hexanoic_acid
2_ethyl_heptanoic_acid
2_propyl_heptanoic_acid
Potency_score
Structural_similarity
Concentration
CYP24A1_11891
CYP26B1_28361
POU4F1_25509
BDNF_25560
GATA2_2599
BMP6_21117
FYN_2527
SEMA6A_10899
ELOVL3_21555
OLFML2A_15337
KRT19_3680
GABBR1_2553
PCDHAC2_4966
CCND2_23334
SYP_11176
NOTCH3_20764
SEMA5A_13118
TUBA1A_12436
ROPN1L_19784
WNT4_15630
CORO1A_1507
MMP9_15866
APLP1_18784
CHST11_28342
KIF5C_3812
TUBB2B_13577
FABP4_21799
EEF1A2_25294
GLI1_19678
ELMOD1_14644
SNAP25_6607
GUCY1B3_11762
CREM_27058
ENO2_13140
NKX2_22301
GAD1_2566
KCNK17_25752
DLL1_16019
SYNGR3_6917
FIBIN_23318
KCNG1_18417
CYP17A1_17310
MT3_20763
SYT1_25933
PRKCH_5429
AMIGO2_19759
G6PD_25228
MAPT_11555
GDPD5_28706
RET_20047

3 Results

3.1 Differentially expressed genes induced by carboxylic acids in PHH can be used to distinguish potent from non-potent responders

To investigate the MoA in response to carboxylic acids in PHH, we performed targeted RNAseq for all compounds at 24 h after exposure in a concentration response (CR) manner. VPA displayed a clear CR in DEGs (Fig. 1A,B) (p-adj < 0.05 & |log-2FC| > 1.5). At the highest concentrations, up to 412 genes were differently expressed, whereas at the lowest concentration only 3 DEGs were observed. The sum of all DEGs in the VPA CR equals 1117, which we named the potency score (PS). By quantifying DEGs for each compound CR, we found that some carboxylic acids showed a CR, whereas others did not. Less potent responders included pivalic acid (PS equals 25 DEGs across the whole CR) and 2-ethylbutyric acid (PS = 441), which are both short-chain carboxylic acids and classified as steatosis-negative. Strong inducers of DEGs included 2-propyl-4-pentenoic acid (PS = 1000), a reactive metabolite of VPA that is known to induce steatosis, and 2-ethyl-hexanoic acid (PS = 928), another well-known steatosis-inducing compound (Escher et al., 2021). Moreover, all three unbranched carboxylic acids, namely propionic, hexanoic and octanoic acid (Tab. 1), caused a CR in the DEGs in PHH (Fig. 1B).

In support of a biological similarity, we anticipated a strong overlap of DEGs in response to different carboxylic acids. When focusing on the middle concentration of 4 mM, we identified some overlapping genes for active responders, but only 6 genes were found to overlap for 14 compounds (Fig. 1C, letter D). Furthermore, 9 genes were unique for 13 compounds (Fig. 1C, letter B). Since most genes were solely found as DEG in single compounds, no obvious gene signature was detected (Fig. 1C).

We hypothesized that PHHs may have the same genes responding to carboxylic acids, but that this response was initiated for a subset of carboxylic acids at a lower concentration. Therefore, we looked at the entire concentration response to determine if overlapping genes are detected at different concentrations. We analyzed the top-50 highest upregulated genes of the 4 mM VPA condition (based on FC with p-adj < 0.05) and looked at the FC of these genes for all compounds across the concentration range. We ranked the compounds by their potency score, expecting to see a similar response in the more potent compounds. Indeed, besides a clear dose response in the top hits for VPA, a very similar response was observed for highly potent carboxylic acids (Fig. 1D). These genes included CYP enzymes, signal transduction proteins (Wnt5a), growth factors (BDNF), apoptosis regulators (CORO1A), and fatty acid metabolism-related proteins (FYN, TUBB2B). Less potent responders, like pivalic acid and ethylbutyric acid, showed an upregulation of these same genes as well, but only at higher concentrations, indicating similarity in MoA despite reduced potency. Finally, we looked at the overlapping genes at the highest concentration (data not shown). No genes were found to overlap for all compounds. However, all analogues, excluding the less potent pivalic acid and 2-ethyl-1-hexanol, had 16 overlapping genes, some of which are mainly involved in cellular stress response pathways (ATF3, CHAC1, CCL2, HAVCR1, DNAJB1, RRM2, HSPA6, ANXA1), lipid metabolism (UGT2A3, NR1D1) or ion channel activity (KCNK1).

3.2 Carboxylic acid exposures provide transcriptomic fingerprints in which potent compounds cluster together

We found highly similar dose responses in the topmost DEGs among potent carboxylic acids, although there was no clear cross-compound gene signature upon 4 mM exposures that could be linked to the AOP for steatosis (Fig. 1C). Also, at the high concentration, a few genes could be linked to a general stress response, but only 2 genes were clearly linked to lipid metabolism. Therefore, an interactive PHH TXG-MAPr tool based on WGCNA, (Callegaro et al., 2021) was used to further explore the transcriptomic datasets beyond the top 50 genes, allowing to derive concentration responses on gene network activation using all (~2,700) genes for 18 compounds. Some gene co-expression modules responded to VPA and were perturbed proportionally to concentration (Fig. 2A). Upregulated modules included PHH:31, PHH:280, PHH:126 and PHH:217, whereas PHH:325 was downregulated by VPA (see Fig. S5[1] for more details about these modules). Next, we compared the highest concentration of potent and less potent carboxylic acid by looking at the Pearson correlation of all module EG scores in the TXG-MAPr (Fig. 2B). The module activation pattern of VPA correlated well with 2-propyl-4-pentenoic acid (Pearson R = 0.91) and significantly less with non-responder pivalic acid (Pearson R = 0.11). By correlating all compounds and all concentrations, potent carboxylic acids correlated well with each other, whereas less potent compounds clustered much less (Fig. 2C, Fig. S3[1]). However, carboxylic acids with a less potent response, like 2-ethylbutyric acid, did cluster with more potent compounds like 2-propylheptanoic acid, suggesting a similar yet weaker biological response in PHHs (Fig. S3[1], cluster 3). Furthermore, even though all unbranched carboxylic acids display a dose response in DEG counts, the higher concentrations do not cluster together based on module EG scores. This finding suggests that compounds with different lengths of unbranched carboxylic acids display a different biological MoA at these high concentrations.

Next, we determined which modules contributed to the similarity of the fingerprint. We focused on the concentration response of modules with |EG score| > 2 and found a similar module activity signature for active compounds. Again, the same modules mentioned before exhibited a dose response (Fig. S4[1]). Even the unbranched carboxylic acids had a higher EG score for our hit modules. So, these modules suggested a fingerprint for carboxylic acid exposure in PHHs and strongly contributed to cluster potent compounds together. This indicated that the MoA of potent compounds was similar but did not yet indicate which underlying biological pathways were affected.

3.3 Module 31 plays a key role in a VPA-like fingerprint and reflects a gene network that represents key events in steatosis

To unravel the biological pathways involved in carboxylic acid exposure, we had a closer look at our hit modules. Module 31 (PHH:31) showed the highest EG scores for VPA as well as other active carboxylic acids with strong module correlation with

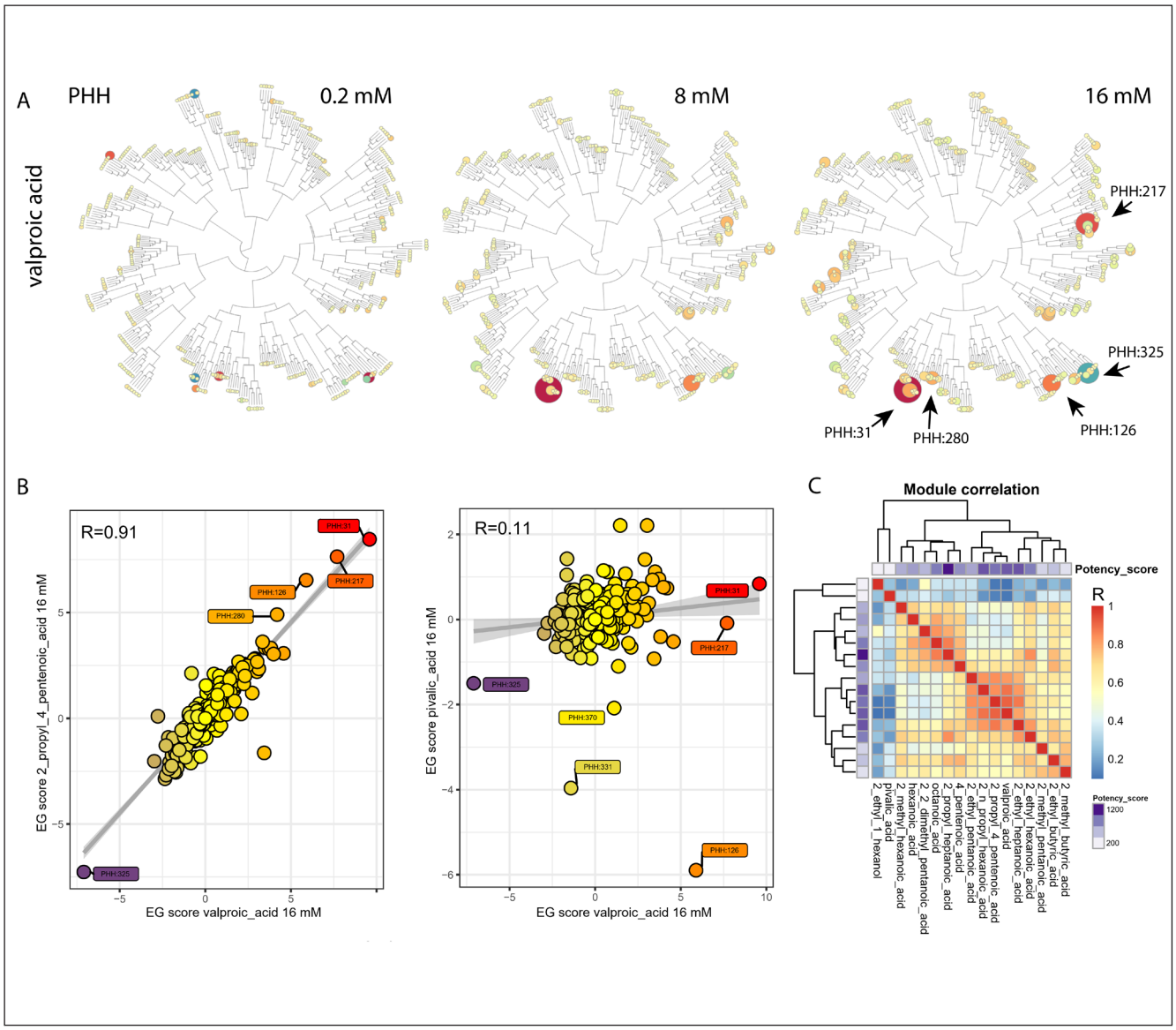

Fig. 2: Toxicogenomics-MAPr correlations for carboxylic acids

A) Application of the TXG-MAPr tool for VPA. Low (0.2 mM), middle (8 mM) and high (16 mM) concentrations are shown. Modules are represented by circles, whose size (small to big, increasing degree of perturbation) and color (blue to red, repression to activation) are proportional to the EG score. Modules that visibly show a dose response are annotated by arrows in the last map. B) Correlation plot of the EG scores of all modules for highly correlated compounds VPA and 2-propyl-4-pentenoic acid (both 16 mM) (Pearson R = 0.91), and for non-correlating compounds pivalic acid and valproic acid (both 16 mM) (Pearson R = 0.11). C) Heatmap showing correlation for all carboxylic acids at 16 mM.

VPA. Therefore, we further evaluated the biological representation of this gene network. PHH:31 displayed a concentration-response activation for carboxylic acids that also had a concentration response in DEGs (Fig. 3A). There are 31 genes involved in PHH:31, seven of which are measured in the S1500+ gene set (Fig. 3B), namely: KIF5C (major role in organelle transport, also regulates SIRT6, which is essential in lipid regulation), GUCY1B3 (main receptor for nitric oxide, which can be induced by VPA), FYN (regulator of fatty acid oxidation), EEF1A2 (promotes GTP-dependent binding of aminoacyl tRNA to ribosomes), TUBB2B (axon guidance and neuronal migration), SLC27A1 (regulating long chain fatty acid substrates during beta-oxidation), and NR1I3 (regulates response elements of CYP enzymes). Interestingly, carboxylic acids that were structurally more similar to VPA had similar EG scores at 1 mM, indicating similar sensitivity (Fig. 3C, left). Annotation based on *in vivo* steatotic potential also demonstrated active carboxylic acids clustering (Fig. 3C, right). When inspecting PHH:31 biological interpretation, gene ontology (GO) terms associated with PHH:31 included fatty acid metabolism and li-

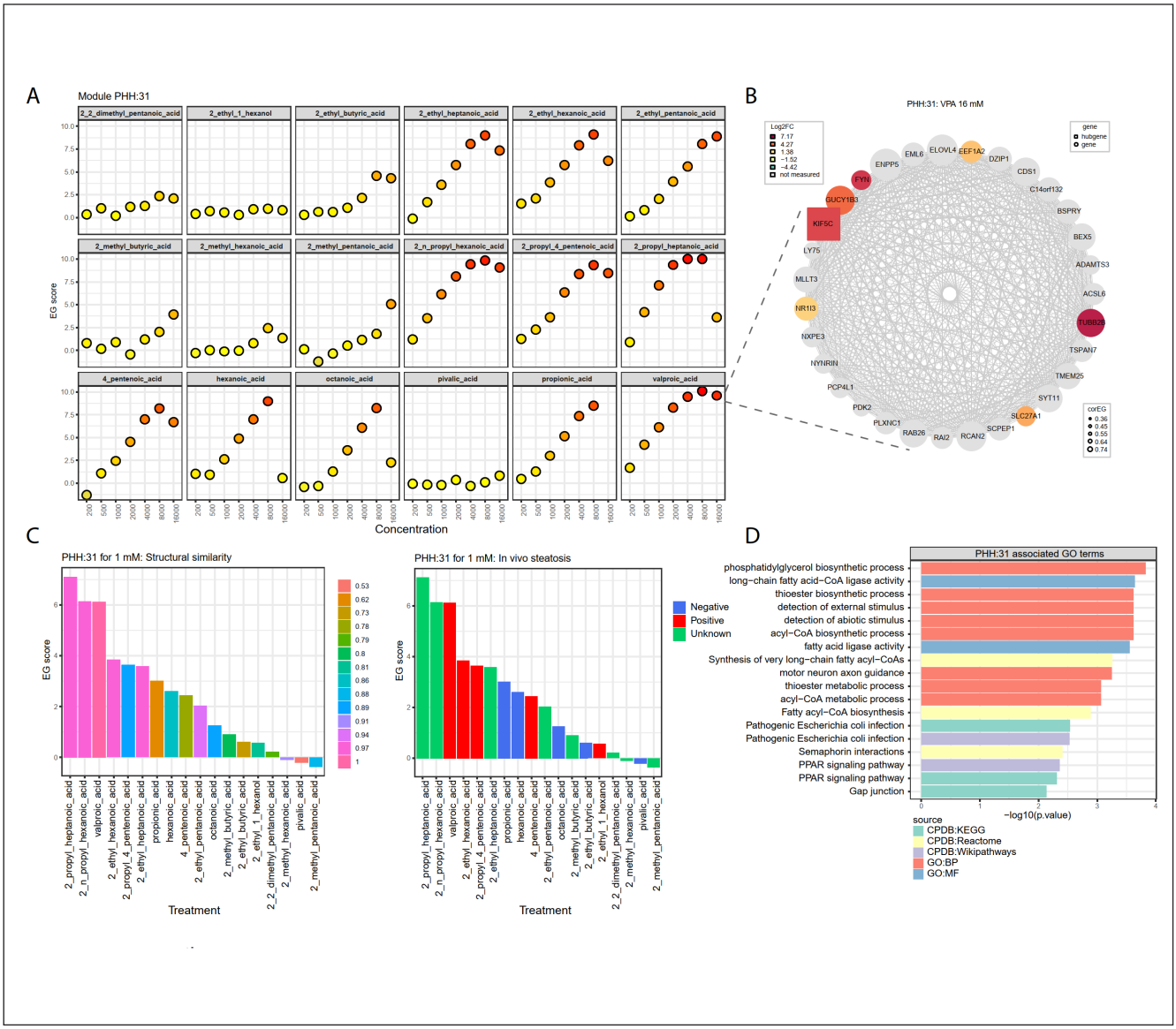

Fig. 3: Concentration response effects on PHH TXG-MAPr module 31 activation by carboxylic acids
A) Dose response plots for PHH:31 for all carboxylic acids. The y-axis shows the EG scores of PHH:31. B) Genes representing PHH:31. Node colors represent fold change, node sizes represent corEG (i.e., how much a gene contributes to the EG score of a module), node shape indicates hub genes. C) Ranking of carboxylic acids based on EG score at 1 mM in module PHH:31. Color represents structural similarity towards VPA (left graph) or steatotic potential *in vivo* (right graph). Carboxylic acids with high structural similarity to VPA have a higher EG score of PHH:31. These compounds are generally also associated with steatosis *in vivo*. D) GO terms associated with PHH:31. Most of the terms are associated with fatty acid metabolism.

gase activities (Fig. 3D). Moreover, PPAR signaling was found to be involved, which is part of the AOP for steatosis. Overall, gene annotation of PHH:31 revealed expected biological terms linked to steatosis, an adverse outcome of VPA exposure.

3.4 Comparison of the whole transcriptome with the S1500+ set on VPA-induced module activation

PHH:31 was critical for carboxylic acid responses, yet for the S1500+ gene panel the overall coverage of PHH:31 was limited to 7 out of 31 genes, including the hub gene. This limited set of genes could pose an uncertainty in using PHH:31 for a read-across assessment. Therefore, we investigated whether a similar response is observed when using the full transcriptome. For a cross-systems comparison, we also evaluated PHH data for VPA from TG-GATEs, which is measured with a microarray platform. Moreover, we determined whether a similar transcriptomics response is observed for HepG2, either using the S1500+ or whole-transcriptome TempO-Seq gene panel. We found that previously identified VPA-responding modules show similar activation patterns compared to TG-GATEs data,

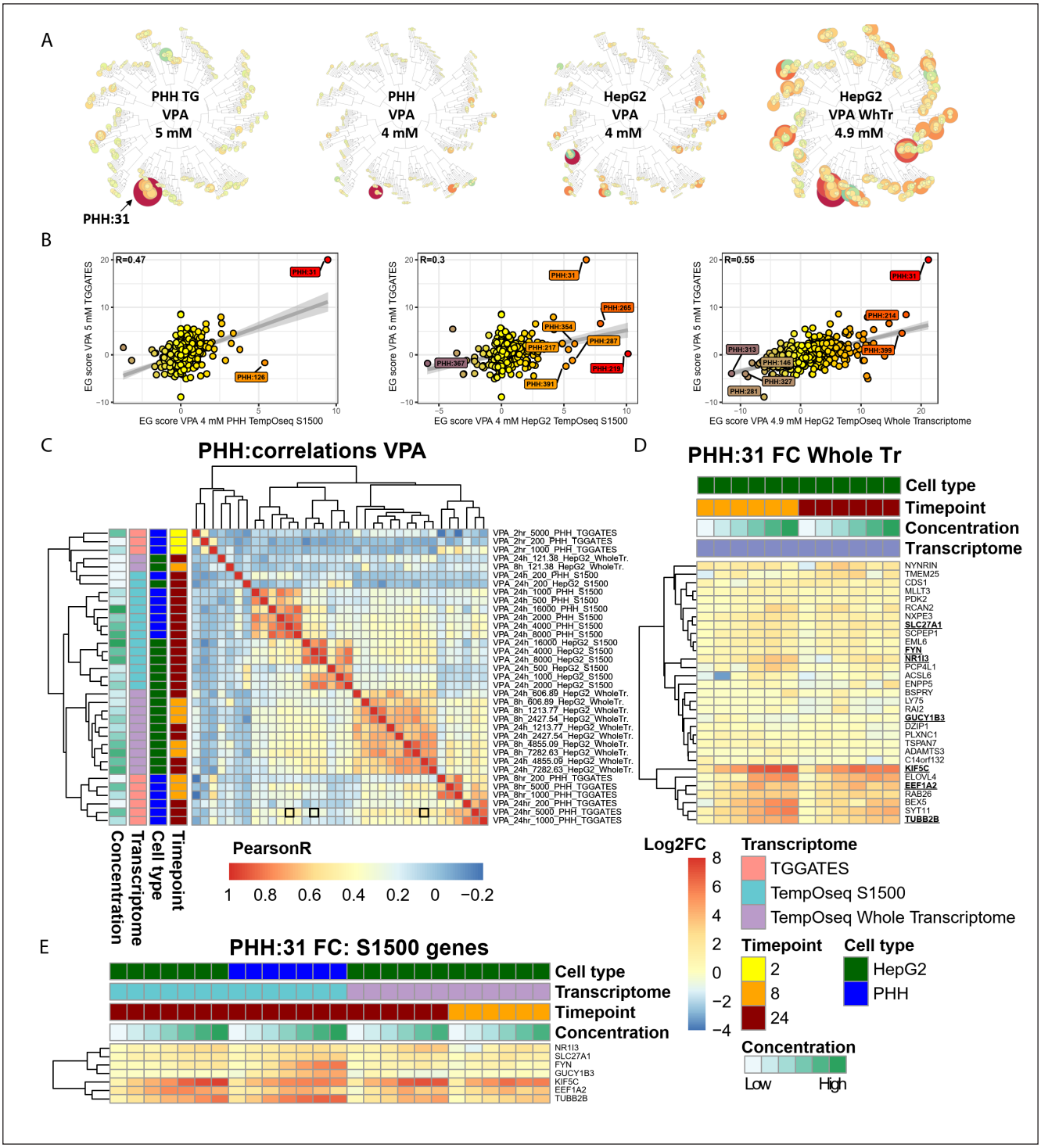

Fig. 4: Comparison of transcriptomic data of liver cells stimulated with VPA

A) TXG-MAP of 24-h VPA-stimulated PHHs of the TG-GATEs, PHHs with TempO-Seq S1500+ EU-ToxRisk panel 2.2, HepG2 cells with TempO-Seq S1500+ EU-ToxRisk panel 2.2, and HepG2 with TempO-Seq whole transcriptome panel. B) Correlation of the EG scores of the highest concentration in the TG-GATEs opposite scores for 4 mM PHHs with the TempO-Seq S1500+ panel, HepG2 with S1500+ panel, and HepG2 with the TempO-Seq whole transcriptome panel. TG-GATES vs TempO-seq S1500: R = 0.47, TG-GATES vs HepG2 TempO-seq: R = 0.3, TG-GATES vs HepG2 Whole Tr.: R = 0.55. C). Module correlation plot of all concentrations and all panels in a concentration range. Black boxes represent the correlations in B. Transcriptome measurements cluster together, especially at the higher concentrations. D) Fold changes of PHH:31 in HepG2 stimulated with VPA in a dose range. Underlined genes are also present in the S1500+ panel. E). Selection of PHH:31 genes that are in the S1500+ panel set, measured for all TempO-Seq experiments.

regardless of the difference in gene set measured and the used transcriptomics platform (Fig. 4A). Naturally, the EG score was lower for the S1500+ panel due to lower coverage of PHH:31 since the module EG score is determined by the log2FC of all genes. The HepG2 cell response to VPA exposure was much stronger as can be appreciated by larger circles representing multiple modules, including PHH:31. When measured at the whole-transcriptome level, the response was even stronger, being the result of the measurement of more genes. Examining the correlation scores, we clearly observed PHH:31 to be strongly activated in all correlation plots, suggesting that this module is a key driver of the VPA regulated response (Fig. 4B). Interestingly, the strongest correlation was observed for 5 mM VPA data in TG-GATEs with whole transcriptome HepG2 data, indicating a better comparison when the whole transcriptome is used. Finally, when correlating all transcriptomic datasets, data from the same cell type and probe set (S1500+ or whole transcriptome) clearly clustered together, indicating the same transcriptomic platform and gene set should be used for cross-compound comparison (Fig. 4C). Next, we observed that the EG score in module 31 for the whole transcriptome for HepG2 was dominated by a subset of genes. Eight genes showed a dose response, of which 4 genes are in the S1500+ panel (Fig. 4D). Since the genes that exhibited a dose response were also present in the S1500+ set, these genes clearly contributed most to the EG score of PHH:31 in the S1500+ panel (Fig. 4D,E). Furthermore, PHHs had even more genes contributing to this module with a dose response for FYN and GUCY1B3, genes that do not contribute in HepG2 (Fig. 4E). So, although the S1500+ set did not cover the whole transcriptome, we were still able to get a reliable fingerprint of VPA by leveraging the PHH TXG-MAPr, allowing reliable MoA determination and comparison with other carboxylic acids for read-across.

3.5 Modest stress response activation in PHH by carboxylic acids

Next, we analyzed the modules that, in addition to PHH:31, were distinctly up- or downregulated upon VPA exposure and treatment with carboxylic acids with similar MoA, including PHH:217, PHH:280, PHH:126 and PHH:325 (Fig. S5[1]). PHH:217 is associated with ion transport, like sodium channel transport and potassium channel regulator activities. Indeed, the MoA of VPA includes blocking sodium channels and T-type calcium channels, which may contribute to its antiepileptic effect (Bourin, 2020). PHH:325 activation, associated with the NRF2 pathway, suggested that the oxidative stress pathway was altered upon VPA exposure. The other two modules had no clear GO terms. However, when we zoomed in on genes involved in PHH:280, we noticed that DDIT3 and HSPA13 were upregulated, both of which are well-known to be involved in the unfolded protein response. PHH:126 displayed regulation of more extracellular matrix functions, like protein binding (NEFL), catenin binding (DSC3), and polysaccharide binding (SBSPON). Given that we found two modules indicating activation of different stress pathways and that the steatosis AOP also contains stress pathway activation, we focused on the stress pathway target gene responses of PHHs to carboxylic acids. We used the DoRothEA database to select genes that are modulated by key stress pathway transcription factors (Fig. 5). Again, we measured similarity in the responses of the most potent carboxylic acids. There was a relatively weak response for the oxidative stress response. For example, SRXN1, a well-known target of NRF2 (Tonelli et al., 2018), was not significantly regulated (data not shown). For other pathways, there was more prominent up- or downregulation of target genes. For instance, for the unfolded protein response, both DDIT3 and PPARGC1A were upregulated. The latter is known to induce PPARG transcription activity as well as PPARD, a known regulator of peroxisomal beta-oxidation of fatty acids. Overall, gene expression in various stress response pathways was perturbed at high concentrations and more strongly by compounds similar to VPA. However, no particular stress pathway was strongly or solely activated, which was also highlighted by the most substantial gene alterations for genes having functions in multiple stress response pathways or cellular processes.

4 Discussion

In this study, we explored the transcriptomic response of PHH cells upon exposure to carboxylic acids that are structurally related to VPA. Some carboxylic acids, including VPA itself, altered transcriptional activity already at low concentrations, whereas others did not – or only minimally – affect gene expression, even at high concentrations (Fig. 1A,B). Overlapping genes at a single concentration did not reveal a clear pathway-related response (Fig. 1C). However, when looking at the entire concentration response, similarities in most susceptible genes among the potent compounds indicated similar MoA (Fig. 1D). This notion was also reflected in the overlapping co-expressed gene modules, including modules 31, 325, 126, 217 and 280 (Fig. 2), all of which are associated with processes known to be modulated by VPA, like fatty acid metabolism, PPAR signaling, ion channel activity, and stress responses (Fig. 3, 5; Fig. S5[1]). Even though our targeted transcriptome panel did not cover all the modules completely (Fig. 4; Fig. S5[1]), our analysis demonstrated that transcriptomic fingerprints can be used to demarcate similarity in MoA of structurally similar chemicals and can, therefore, support read-across approaches in the context of toxicity assessment.

Chemical read-across commonly lacks information on the biological MoA, yet still relies on the premise that structurally similar compounds yield similar toxicological profiles. Nowadays, toxicity testing aims to employ the richness of omics data integration to establish an understanding of mechanisms underlying toxicity as an adverse outcome, and read-across studies are performed with toxicogenomics datasets such as TG-GATEs, DrugMatrix, Connectivity Map, and LINCS1000 (Serra et al., 2020). Here, we performed a systematic transcriptomics-driven biological similarity analysis using a panel of 18 structurally similar VPA analogues. By combining both physicochemical (i.e., structural similarity) and biological (i.e., transcriptomics) data, we found that indeed VPA-like compounds with a high similarity have a similar transcriptomic re-

A

Stress response pathway	Transcription factors	# Targets genes ABC confidence	# Genes in ABC in EUToxRisk panel
Oxidative stress	NFE2L2	72	26
Unfolded protein response	ATF4, ATF6, XBP1	142	49
DNA damage	TP53	600	197
Inflammation	NFKB1, NFKB2, REL, RELA, RELB	637	192

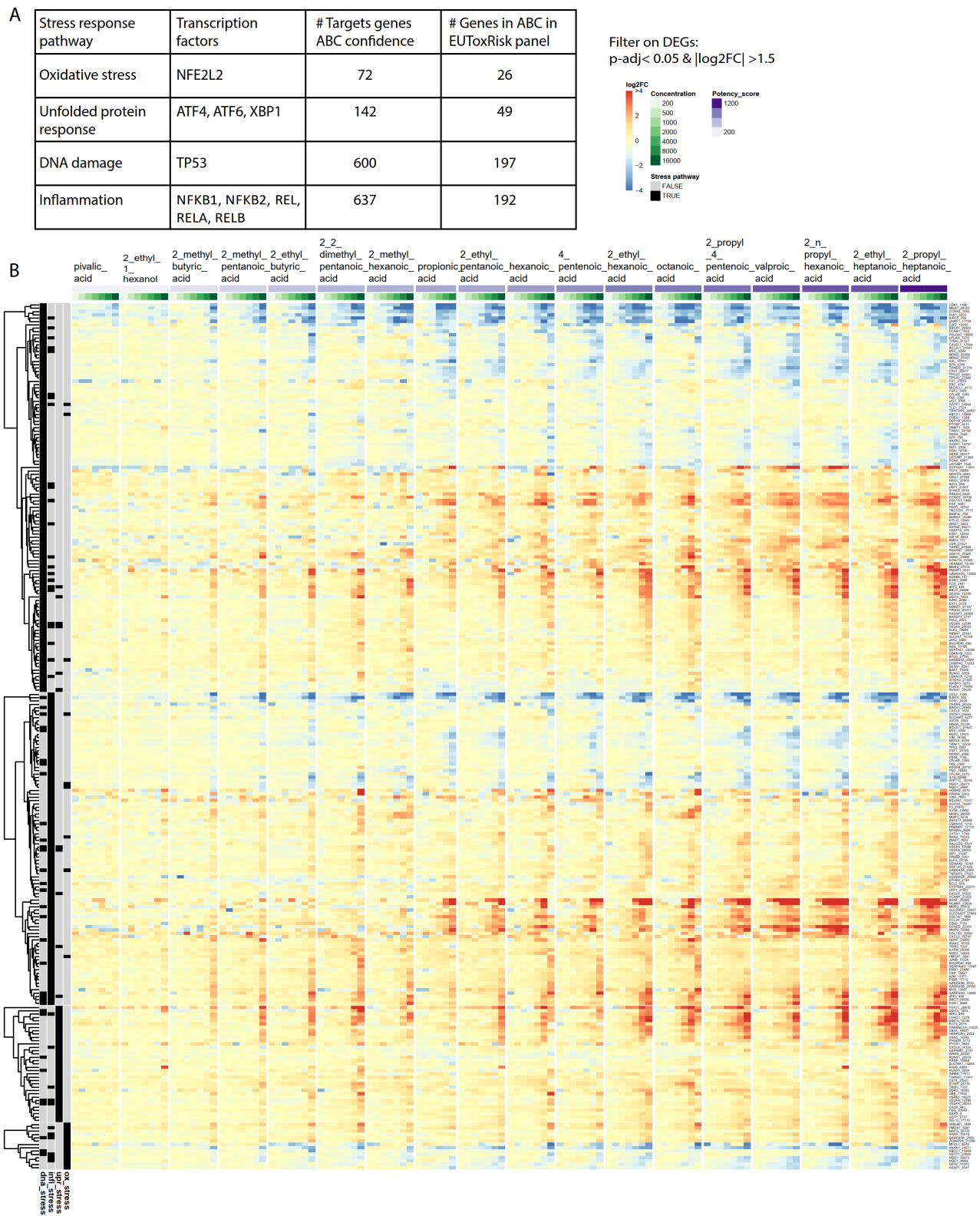

Fig. 5: Stress response activation by carboxylic acids

A) Chosen transcription factors for stress pathways and number of genes filtered. Annotation of heatmap. B) Heatmap of stress response genes. Left bar indicates to which pathway a probe belongs. Euclidean clustering is applied per pathway.

sponse in overall gene expression as well as potency. In contrast, pivalic acid, with the lowest similarity score, had no response at all at the highest concentration studied, indicating far lower potency and/or different MoA relative to VPA. Compounds with a higher similarity score than pivalic acid but lower than octanoic acid and 2-propyl-4-pentenoic acid showed a varying potency in concentration responses on both gene FC levels as well as in the number of DEGs. Thus, there is no overall linear relationship between potency and structural similarity. We cannot exclude that these discrepancies are related to differences in toxicokinetic properties of the carboxylic acid analogues in PHHs. Regardless, despite the differences in potency, all carboxylic acids with a transcriptomics potency score > 628, based on the sum of all the DEGs across the concentration range, had a similar gene expression profile when comparing to top-50 genes upregulated by VPA.

Additionally, we established a transcriptomic gene-network fingerprint and found clear correlations among potent carboxylic acids. The highest gene module EG score was found for PHH:31, associated with PPAR signaling and acyl-CoA metabolism, both well-known processes in the mechanisms of VPA toxicity and steatogenesis (Silva et al., 2008; Szalowska et al., 2014). Indeed, PPAR signaling is a key event in the AOP for chemical-induced liver steatosis, just like inhibition of beta-oxidation, an essential pathway in acyl-CoA metabolism (Landesmann et al., 2012; van Breda et al., 2018). Integration of the S1500+ TempO-Seq panel with the TXG-MAPr turned out to be a high-throughput and cost-effective approach to derive quantitative biological read-across information on relevant toxicological responses. Indeed, the S1500+ gene set is a good alternative for whole transcriptome analysis (Callegaro et al., 2021). To corroborate this further, we compared this panel with whole transcriptome targeted sequencing and the TG-GATEs data and found that key genes responsible for module activation were indeed present in the S1500+ panel. Low correlation scores of the transcriptomic fingerprint of VPA measured by different numbers of genes (S1500+ vs whole transcriptome) can be explained by the lower EG scores of modules due to lower module gene coverage, since the module EG score is a combination score of log2FC for all genes that are present. Nevertheless, the module fingerprint for VPA and carboxylic acids was clearly determined by PHH:31, which also represented the expected biological interpretation. The user-friendly interface of the TXG-MAPr tool and the visualization of DEG data were ideal for revealing a shared mode-of-action, which contributes to a mechanism-based read-across of carboxylic acids. We successfully used the quantitative responses of biologically annotated modules, such as PHH:31, to compare the *in vitro* benchmark concentrations of carboxylic acids for the most sensitive biological response. Thus, we anticipate that this approach is fit to provide biological information for read-across. Given the mechanistic insights from the gene-network modules, this would also allow a suitable link to key events in an AOP.

Since classical read-across and toxicity assessment use animal studies, we compared the *in vivo* endpoint steatosis, an adverse outcome of VPA-induced hepatotoxicity in rodents and humans, with our gene expression profiles. In both FC data and EG scores, steatosis-positive compounds clustered together at higher concentrations, except for 2-ethyl-1-hexanol, which can induce steatosis in animals but did not display a response in PHHs. We speculate that oxidation of this carboxylic acid may not take place to the same extent as observed in *in vivo* studies. Furthermore, unbranched carboxylic acids also induced transcriptomic responses that were similar to those in response to VPA, although less prominent. Indeed, SCFA (e.g., propionic acid) and MCFA (e.g., hexanoic and octanoic acid) are also HDAC inhibitors like VPA and can interfere with inflammatory pathways via FFAR2/3 and play a role in lipid metabolism (He et al., 2020). But, in contrast to VPA, these compounds did not induce steatosis *in vivo* (Szilagyi, 2012). This can be explained by the way SCFA and MCFA are metabolized. Both can pass into mitochondria passively to enter the fatty acid oxidation process (Knottnerus et al., 2018), whereas VPA needs to be actively transported by carnitine, thereby interfering with the metabolism of long-chain fatty acids (Silva et al., 2008). Silva et al. (2008) described several mechanisms by which VPA can induce hepatotoxicity, including formation of reactive metabolites, drug-induced co-enzyme A depletion, carnitine deficiency, and oxidative stress. Since SCFA and MCFA also use co-enzyme A in lipid metabolism and induce oxidative stress according to this study (even more so than VPA), it is likely that carnitine deficiency is a main contributor of hepatosteatosis. Metabolomics analysis could therefore be a valuable addition to provide further biological support in read-across studies.

Here we showed that changes at the expressed genome level can help evaluate a shared MoA in a qualitative way and point toward differences in potency within structurally similar carboxylic acids. Nonetheless, for a complete read-across, which includes the derivation of a threshold value, one still requires additional readouts closer to the adverse outcome, as not all early events might progress to late key events (Escher et al., 2021). In this case, the accumulation of triglycerides in hepatocytes is, for example, a suitable late KE close to the adverse outcome liver steatosis.

In summary, we found that structurally related carboxylic acids had similar toxicological profiles, especially for compounds that show the highest structural similarity. Transcriptomics is one essential building block in biological similarity assessment and contributes to hazard identification. Tools like the TXG-MAPr have a great potential to visualize biological similarities at the gene level and could be an integral part of similarity assessment. When modules are more completely mapped to pathological outcomes, we may be able to better predict the adverse outcomes based on transcriptomics. Since safety sciences are moving away from animal studies in risk assessment, targeted transcriptomics is likely to become a significant tool for underpinning *in vivo* toxicity data. Mapping transcriptomics onto AOPs delivers a mechanistic understanding that is key to IATA.

References

Abdel-Dayem, M. A., Elmarakby, A. A., Abdel-Aziz, A. A. et al. (2014). Valproate-induced liver injury: Modulation by the omega-3 fatty acid DHA proposes a novel anticonvulsant regimen. *Drugs R D 14*, 85-94. doi:10.1007/s40268-014-0042-z

Acosta Jr, D. (2012). Pharmaceuticals. In E. Bingham and B. Cohrssen (eds.), *Patty's Toxicology* (583-602). John Wiley & Sons, Inc. doi:10.1002/9780471125471.tox001.pub2

Baillie, T. A. (1992). Metabolism of valproate to hepatotoxic intermediates. *Pharm Weekbl Sci Ed 14*, 122-125. doi:10.1007/BF01962701

Bourin, M. (2020). Mechanism of action of valproic acid and its derivatives. *SOJ Pharm Pharm Sci 7*, 1-4. doi:10.15226/2374-6866/7/1/00199

Callegaro, G., Kunnen, S. J., Trairatphisan, P. et al. (2021). The human hepatocyte TXG-MAPr: Gene co-expression network modules to support mechanism-based risk assessment. *Arch Toxicol 95*, 3745-3775. doi:10.1007/s00204-021-03141-w

Escher, S. E., Kamp, H., Bennekou, S. H. et al. (2019). Towards grouping concepts based on new approach methodologies in chemical hazard assessment: The read-across approach of the EU-ToxRisk project. *Arch Toxicol 93*, 3643-3667. doi:10.1007/s00204-019-02591-7

Escher, S. E., Aguayo-Orozco, A., Benfenati, E. et al. (2021). A read-across case study on chronic toxicity of branched carboxylic acids (1): Integration of mechanistic evidence from new approach methodologies (NAMs) to explore a common mode of action. *Toxicol In Vitro 79*, 105269. doi:10.1016/j.tiv.2021.105269

Espandiari, P., Zhang, J., Schnackenberg, L. K. et al. (2008). Age-related differences in susceptibility to toxic effects of valproic acid in rats. *J Appl Toxicol 28*, 628-637. doi:10.1002/jat.1314

Garcia-Alonso, L., Holland, C. H., Ibrahim, M. M. et al. (2019). Benchmark and integration of resources for the estimation of human transcription factor activities. *Genome Res 29*, 1363-1375. doi:10.1101/gr.240663.118

Gwinn, W. M., Auerbach, S. S., Parham, F. et al. (2020). Evaluation of 5-day in vivo rat liver and kidney with high-throughput transcriptomics for estimating benchmark doses of apical outcomes. *Toxicol Sci 176*, 343-354. doi:10.1093/toxsci/kfaa081

Harrill, J. A., Everett, L. J., Haggard, D. E. et al. (2021). High-throughput transcriptomics platform for screening environmental chemicals. *Toxicol Sci 181*, 68-89. doi:10.1093/toxsci/kfab009

He, J., Zhang, P., Shen, L. et al. (2020). Short-chain fatty acids and their association with signalling pathways in inflammation, glucose and lipid metabolism. *Int J Mol Sci 21*, 6356. doi:10.3390/ijms21176356

Huppelschoten, S. (2017). *Dynamics of TNFalpha Signaling and Drug-Related Liver Toxicity*. Leiden University.

Ibrahim, M. A. (2012). Evaluation of hepatotoxicity of valproic acid in albino mice, histological and histoistochemical studies. *Life Sci J 9*, 153-159. https://www.researchgate.net/publication/285774185

Juberg, D. R., David, R. M., Katz, G. V. et al. (1998). 2-ethylhexanoic acid: Subchronic oral toxicity studies in the rat and mouse. *Food Chem Toxicol 36*, 429-436. doi:10.1016/S0278-6915(97)00168-3

Kavlock, R. J., Bahadori, T., Barton-Maclaren, T. S. et al. (2018). Accelerating the pace of chemical risk assessment. *Chem Res Toxicol 31*, 287-290. doi:10.1021/acs.chemrestox.7b00339

Knapp, A. C., Todesco, L., Beier, K. et al. (2008). Toxicity of valproic acid in mice with decreased plasma and tissue carnitine stores. *J Pharmacol Exp Ther 324*, 568-575. doi:10.1124/jpet.107.131185

Knottnerus, S. J. G., Bleeker, J. C., Wüst, R. C. I. et al. (2018). Disorders of mitochondrial long-chain fatty acid oxidation and the carnitine shuttle. *Rev Endocr Metab Disord 19*, 93-106. doi:10.1007/s11154-018-9448-1

Landesmann, B., Gomenou, M., Munn, S. et al. (2012). Description of Prototype Modes-of-Action Related to Repeated Dose Toxicity. EUR 25631 EN. Luxembourg (Luxembourg): Publications Office of the European Union. JRC75689. doi:10.2788/71112

Limonciel, A., Ates, G., Carta, G. et al. (2018). Comparison of base-line and chemical-induced transcriptomic responses in HepaRG and RPTEC/TERT1 cells using TempO-Seq. *Arch Toxicol 92*, 2517-2531. doi:10.1007/s00204-018-2256-2

Löscher, W., Wahnschaffe, U., Hönack, D. et al. (1992). Effects of valproate and E-2-en-valproate on functional and morphological parameters of rat liver. I. Biochemical, histopathological and pharmacokinetic studies. *Epilepsy Res 13*, 187-198. doi:10.1016/0920-1211(92)90052-U

Love, M. I., Huber, W. and Anders, S. (2014). Moderated estimation of fold change and dispersion for RNA-seq data with DESeq2. *Genome Biol 15*, 550. doi:10.1186/s13059-014-0550-8

Mav, D., Shah, R. R., Howard, B. E. et al. (2018). A hybrid gene selection approach to create the S1500+ targeted gene sets for use in high-throughput transcriptomics. *PLoS One 13*, e0191105. doi:10.1371/journal.pone.0191105

Patlewicz, G., Kuseva, C., Kesova, A. et al. (2014). Towards AOP application – Implementation of an integrated approach to testing and assessment (IATA) into a pipeline tool for skin sensitization. *Regul Toxicol Pharmacol 69*, 529-545. doi:10.1016/j.yrtph.2014.06.001

Pistollato, F., Madia, F., Corvi, R. et al. (2021). Current EU regulatory requirements for the assessment of chemicals and cosmetic products: Challenges and opportunities for introducing new approach methodologies. *Arch Toxicol 95*, 1867-1897. doi:10.1007/s00204-021-03034-y

Ramaiahgari, S. C., Auerbach, S. S., Saddler, T. O. et al. (2019). The power of resolution: Contextualized understanding of biological responses to liver injury chemicals using high-throughput transcriptomics and benchmark concentration modeling. *Toxicol Sci 169*, 553-566. doi:10.1093/toxsci/kfz065

Robinson, M. D., McCarthy, D. J. and Smyth, G. K. (2010). edgeR: A Bioconductor package for differential expression analysis of digital gene expression data. *Bioinformatics 26*, 139-140. doi:10.1093/bioinformatics/btp616

Rovida, C., Escher, S. E., Herzler, M. et al. (2021). NAM-supported read-across: From case studies to regulatory guidance in safety assessment. *ALTEX 38*, 140-150. doi:10.14573/altex.2010062

Schultz, T. W., Amcoff, P., Berggren, E. et al. (2015). A strategy for structuring and reporting a read-across prediction of toxicity. *Regul Toxicol Pharmacol 72*, 586-601. doi:10.1016/j.yrtph.2015.05.016

Semino, G. (1998). Saturated aliphatic acyclic branched-chain primary alcohols, aldehydes, and acids. WHO, Geneva. http://www.inchem.org/documents/jecfa/jecmono/v040je11.htm

Serra, A., Fratello, M., Cattelani, L. et al. (2020). Transcriptomics in toxicogenomics, part III: Data modelling for risk assessment. *Nanomaterials 10*, 708. doi:10.3390/nano10040708

Silva, M. F. B., Aires, C. C. P., Luis, P. B. M. et al. (2008). Valproic acid metabolism and its effects on mitochondrial fatty acid oxidation: A review. *J Inherit Metab Dis 31*, 205-216. doi:10.1007/s10545-008-0841-x

Sugimoto, T., Woo, M., Nishida, N. et al. (1987). Hepatotoxicity in rat following administration of valproic acid. *Epilepsia 28*, 142-146. doi:10.1111/j.1528-1157.1987.tb03640.x

Szalowska, E., Van Der Burg, B., Man, H. Y. et al. (2014). Model steatogenic compounds (amiodarone, valproic acid, and tetracycline) alter lipid metabolism by different mechanisms in mouse liver slices. *PLoS One 9*, e86795. doi:10.1371/journal.pone.0086795

Szilagyi, M. (2012). Aliphatic carboxylic acids: Saturated. In E. Bingham and B. Cohrssen (eds.), *Patty's Toxicology* (471-532). John Wiley & Sons, Inc. doi:10.1002/9780471125471.tox001.pub2

Tang, W., Borel, A. G., Abbott, F. S. et al. (1995). Fluorinated analogues as mechanistic probes in valproic acid hepatotoxicity: Hepatic microvesicular steatosis and glutathione status. *Chem Res Toxicol 8*, 671-682. doi:10.1021/tx00047a006

Thayer, W. S. (1984). Inhibition of mitochondrial fatty acid oxidation in pentenoic acid-induced fatty liver. A possible model for Reye's syndrome. *Biochem Pharmacol 33*, 1187-1194. doi:10.1016/0006-2952(84)90169-2

Tollefsen, K. E., Scholz, S., Cronin, M. T. et al. (2014). Applying adverse outcome pathways (AOPs) to support integrated approaches to testing and assessment (IATA). *Regul Toxicol Pharmacol 70*, 629-640. doi:10.1016/j.yrtph.2014.09.009

Tonelli, C., Chio, I. I. C. and Tuveson, D. A. (2018). Transcriptional regulation by Nrf2. *Antioxid Redox Signal 29*, 1727-1745. doi:10.1089/ars.2017.7342

Tong, V., Teng, X. W., Chang, T. K. H. et al. (2005). Valproic acid I: Time course of lipid peroxidation biomarkers, liver toxicity, and valproic acid metabolite levels in rats. *Toxicol Sci 86*, 427-435. doi:10.1093/toxsci/kfi184

van Breda, S. G. J., Claessen, S. M. H., van Herwijnen, M. et al. (2018). Integrative omics data analyses of repeated dose toxicity of valproic acid in vitro reveal new mechanisms of steatosis induction. *Toxicology 393*, 160-170. doi:10.1016/j.tox.2017.11.013

Vinken, M. (2015). Adverse outcome pathways and drug-induced liver injury testing. *Chem Res Toxicol 28*, 1391-1397. doi:10.1021/acs.chemrestox.5b00208

Wickham, H. (2007). Reshaping data with the {reshape} package. *J Stat Softw 21*, 1-20. doi:10.18637/jss.v021.i12

Yang, H., Niemeijer, M., van de Water, B. et al. (2020). ATF6 is a critical determinant of CHOP dynamics during the unfolded protein response. *iScience 23*, 100860. doi:10.1016/j.isci.2020.100860

Yeakley, J. M., Shepard, P. J., Goyena, D. E. et al. (2017). A trichostatin A expression signature identified by TempO-Seq targeted whole transcriptome profiling. *PLoS One 12*, e0178302. doi:10.1371/journal.pone.0178302

Yuge, K. (1990). Carnitine metabolism in rats with 4-pentenoic acid induced fatty liver. *Pediatr Int 32*, 449-455. doi:10.1111/j.1442-200X.1990.tb00859.x

Conflict of interest

The authors declare that they have no conflicts of interest.

Acknowledgements

This project has received funding from the European Union's Horizon 2020 research and innovation programme under grant agreement No. 681002 (EU-ToxRisk), the Innovative Medicine Initiative TransQST project (grant No. 116030), eTRANSAFE project (grant number 777365), and the Ontology project supported by the Cosmetics Europe and Cefic research programmes.